

# Taking into Account the Shell Finite Element Size for Computing the Reinforcement of a Monolithic Floor

Rusakov, A.I.

It is suggested the technique of computing the reinforcement of floors of a monolithic skeleton in vicinity of columns. In the technique it is applied the results of computing the reinforcement in linear-elastic model with slab's support on the column in a single node. The reinforcement area is defined more precisely by taking into consideration nonlinear properties of armored concrete and given cross-sections of the columns.

## 1. Introduction

Let us consider a typical finite element (FE) structure of multistorey reinforced concrete frame including a mat foundation, smooth (unbeamed) floors and a system of vertical elements — stiffening diaphragms and columns. In slabs' modeling to define stress-strained state (SSS) for the reinforcement, one uses FE of thin linear-elastic shell with prevailing square 4-nodes elements; in columns' modeling one uses linear-elastic beam elements. The conjunction of a floor or foundation slab with a

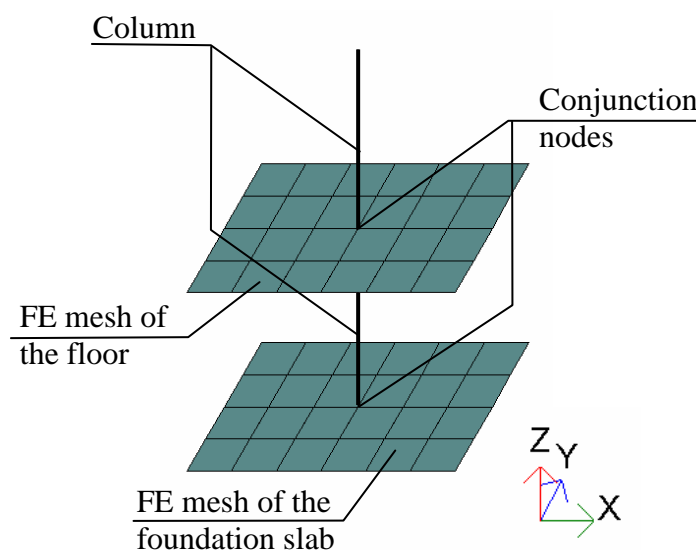


Fig. 1

column is secured by a common node of corresponding elements (Fig.1). Under such modeling of bindings of a slab and a column the conjunction node is the origin of concentrated force upon the slab from the column. This means that in the analytical model of a slab, under which slab is supposed to be a linear-elastic shell with concentrated forces applied to points of columns' supports, on the decrease of a distance to this points there increases shearing force and bending moments up to infinity.

The general technique of estimation of reinforcement sectional area for a slab in the vicinity of columns is that of reinforcement's calculation for all the shell FEs, using slab SSS defined by linear computing, with choosing of the element that has greatest reinforcement area of ones contacting to the column. This greatest area is considered to be reinforcement intensity of given direction in the additional reinforcement region near the support. In this concept, on the decrease of step of finite-element mesh (FE mesh), the greatest bending moments  $M_x$  and  $M_y$  increases up infinitely and, as result, there increases calculated reinforcement area.

The scheme described above (of estimation of positive-moment reinforcement) we shall name as a scheme of reinforcement-on-point-support calculation. When applying this scheme structural designer assumes reinforcement adequacy under suitable step of FE mesh. Yet there is no reliable recommends of choosing shell FE size. Besides that, the results presented below point out that reinforcement calculation error depends both on the FE mesh and cross-section size of given column. In this paper we propose to complete the scheme of reinforcement on point support by introduction of coefficients of recalculation of positive-moment reinforcement obtained by a common algorithm. Under given conditions of reinforcement (in particular, given negative-moment reinforcement area) it is suggested to determine the recalculation coefficients  $\alpha_x, \alpha_y$ , by which we derive the positive-moment reinforcement area at the site of support:

$$A_{x(y)} = \alpha_{x(y)} A_{x(y)}^{ps},$$

where  $A_{x(y)}^{ps}$  is the area of sectional reinforcement on the point support of  $x$  or  $y$  direction. In the paper we present the technique of tabulation of coefficients under consideration to specify the relation:

$$\alpha_{x(y)} = \alpha_{x(y)}(l, B, H, A_{x(y)}^{ps}), \quad (1)$$

where  $l$  is the FE mesh's step as before;  $B$  is the column's cross-section dimension of  $x$  direction in the global coordinate system ("width" of section);  $H$  is the column's cross-section dimension of  $y$  direction in the global coordinate system ("height" of section). About negative-moment reinforcement area it is assumed that one is equal to basic ("background") reinforcement area. The technique is adapted to the computing suit LIRA 9.2.

## 2. Technique main regulations

In the technique of coefficients  $\alpha_{x(y)}$  computation there are suggested next source data: slab width  $h$ ; clear distance from upper and lower longitudinal reinforcement to corresponding face of slab; concrete and reinforcement classes and corresponding stress-strain diagrams of tension and compression; concrete behavior and reinforcement behavior coefficients; upper limit of positive-moment reinforcement area on point support for the skeleton of building  $A_{\max}^{ps}$ ; negative-moment reinforcement area at the site of support  $A'_y$  under assumption  $A'_x = A'_y$  (the second-order character points to the reinforcement direction); parameters  $l, B, H$ . Besides, it is specified the boundaries for bending moments in the vicinity of slab supports, that caused by the loads of various types in the skeleton of a given typical structure. Further we set forth the technique for the case of a slab with a given width  $h$ , of given parameters  $l, B$ , and of square cross-section of a column. Then the technique is generalized for rectangular section of a column. The stages of coefficients  $\alpha_{x(y)}$  computation are as follows:

1. Complete the finite-element model (FE model) of reinforcement on point

support that approximately represents possible cases of support displacement inside the slab's plan. In the simple analytical model a square slab supported in its center is loaded with uniform pressure  $\tilde{q}$  (Fig. 2, a). Determine the positive-moment reinforcement area  $\tilde{A}_y^{ps}$  as a tabulated function of load  $\tilde{q}$ :

$$\tilde{A}_y^{ps} = A_y^{ps}(\tilde{q}) \quad (2)$$

(in the case under consideration owing to symmetry we have  $\tilde{A}_x^{ps} = \tilde{A}_y^{ps}$ ).

2. Complete the nonlinear-elastic FE model of reinforcement on plain support with analytical model of previous stage. In the latter FE model the dimensions of plain support are equal to cross-sectional dimensions of a given column and FE is of a small size and of reinforcement determined on the former stage. Model is intended to determine the extreme load  $q$  for reinforcement area  $A_x = A_y = \tilde{A}_y^{ps}$ , defined for any  $\tilde{q}$  by the table composed on former stage. The model implements the stepwise algorithm of construction loading [1, subsect. 3.5], that fixes the load of destruction  $q$ . After determination of extreme load, it is estimated the crack separation distance in marginal state. As a result of stage it is accomplished the tabulated relation of destructive loads:

$$q = q(A_y). \quad (3)$$

3. Match the reinforcement area on the point support for each destructive load  $q$  obtained at the stage 2:

$$A_y^{ps} = A_y^{ps}(q). \quad (4)$$

Calculate search coefficient

$$\alpha_x = \alpha_y = \frac{A_y}{A_y^{ps}}. \quad (5)$$

Completing the stage, make transition in the relation  $\alpha_{x(y)} = \alpha(q)$  from the argument  $q$  to argument  $A_y^{ps}$  through the function inverse to function (2); plot the graphic chart of function

$$\alpha_y = \alpha_y(A_y^{ps}). \quad (6)$$

Remark. Tabulated function (2) gives the rough estimation of destruction load  $\tilde{q} \approx q$  under  $A_x = A_y = \tilde{A}_y^{ps}$ . Without such estimation we can't construct an algorithm of seeking the function (3).

4. Check usability of the function (6) for reinforcement calculation in special cases of slab loading:

A) check the accuracy of coefficients  $\alpha_y$  calculation under the loading of partitioning wall and area load together;

B) check the accuracy of coefficients  $\alpha_y$  calculation for station of a column on a slab verge;

C) check the accuracy of coefficients  $\alpha_y$  calculation for station of a column on a slab corner.

For each checking A—B we have to compile corresponding model based on nonlinear-elastic reinforced elements.

**The technique described is based on the assumption that coefficient  $\alpha_y = \alpha_y(A_y^{ps})$  established by means of developed models for given argument  $A_y^{ps}$ , is equal to the ratio of required reinforcement area over reinforcement area on point support in actual monolithic skeleton (besides, in account of square cross-section of a column, similar relationship takes place for the reinforcement of  $x$ -direction).**

3. The example of  $\alpha$ -coefficients calculation and numerical results of the paper

Let us consider the floor of width  $h = 20$  cm of civic building and establish coefficients  $\alpha$  for FE of a size  $l = 50$  cm and for a column of section 50×50 cm. The specific of construction is: the greatest span of 6.5 m; walling makes the loading 1250 kgs/m; the greatest loading of partitions is of 400 kgs/m. We propose class of concrete B25, class of reinforcement A-III, the distance from upper and lower longitudi-

nal reinforcement to nearest face of slab  $a = a' = 3$  cm, the crack separation distance and material behavior coefficients is specified in accordance with SNIP 2.03.01-84\*, the upper limit of stretched longitudinal reinforcement on point support for a given skeleton is  $A_{\max}^{ps} = 22$  cm<sup>2</sup>/m; the area of compressed longitudinal reinforcement in the support site is  $A'_{x(y)} = 2$  cm<sup>2</sup>/m. The analytical model for FE-modeling of the slab is the table supported on the column (Fig. 2, a).

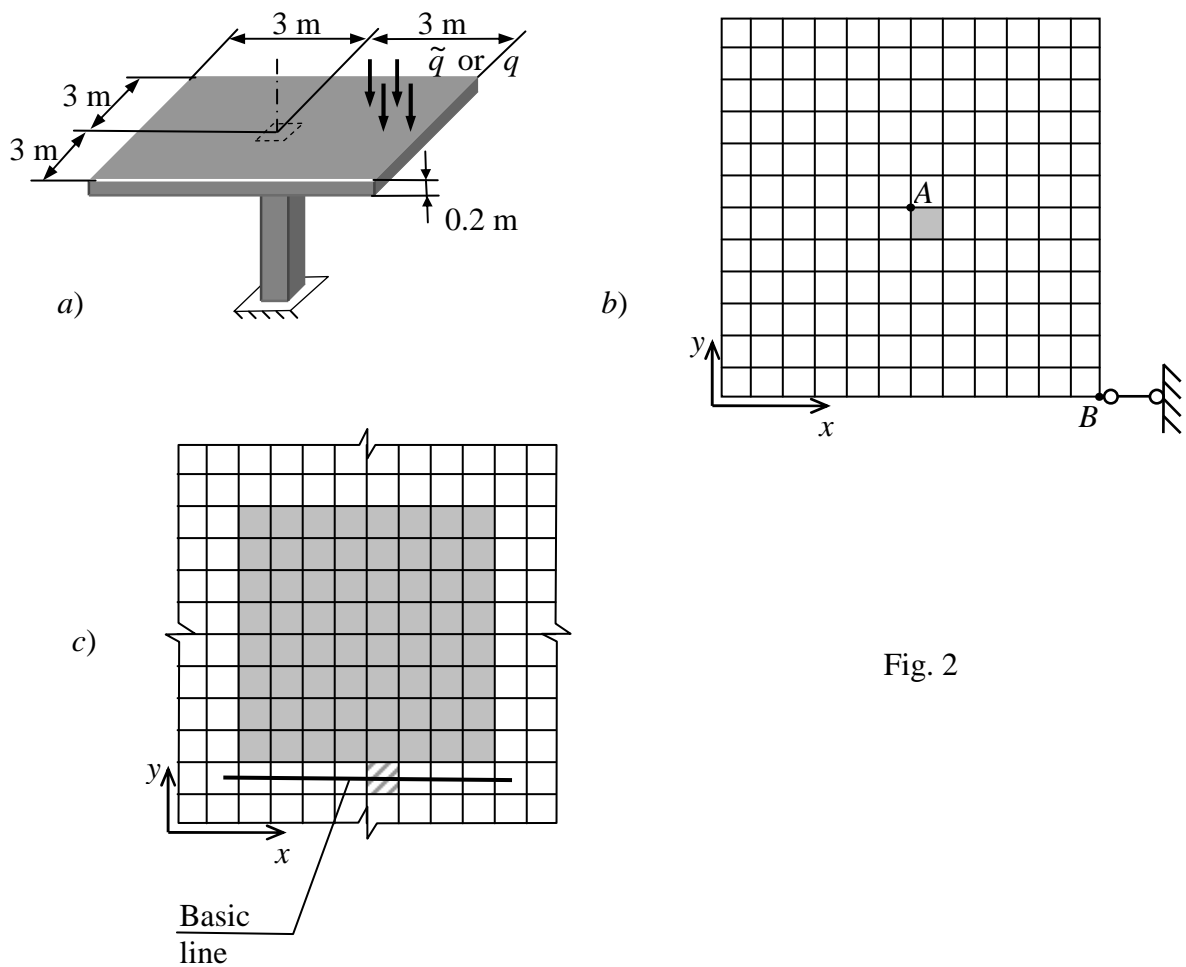


Fig. 2

The FE mesh of reinforcement on point support is depicted on Fig. 2, b. Node A represents the support on the column and has 6 restraints (translational and angular). Node B secures invariability of the system and has 1 restraint depicted on the scheme. The mesh step is  $l = 50$  cm. That element by which the reinforcement on point support has been established is marked with filling. The results of model analysis are presented in columns 1—2 of Table 1.

The sub-image of FE mesh on plain support is depicted on Fig. 2, *c*; mesh step  $l = 6.25$  cm. The region of bearing nodes is selected by filling. The basic line has been traced through those elements, which the crack separation is estimated by.

Table 1

$\tilde{q}$ , ton/m <sup>2</sup>	$\tilde{A}_y^{ps} =$ $= A_y$ , cm <sup>2</sup> /m	$k$	$k\tilde{q}$ , ton/m <sup>2</sup>	$q$ , ton/m <sup>2</sup>	$A_y^{ps}$ , cm <sup>2</sup> /m	$\alpha_{x(y)}$
0.5	5.51	1.2	0.6	0.5314	5.87	0.939
0.65	7.27	1.2	0.78	0.6386	7.13	1.020
0.8	9.09	1.1	0.88	0.7242	8.16	1.114
1	11.63	1	1	0.8445	9.65	1.205
1.2	14.31	0.9	1.08	0.9677	11.21	1.277
1.4	17.15	0.9	1.26	1.1550	13.69	1.253
1.5	18.65	0.9	1.35	1.2723	15.32	1.217
1.6	20.20	0.9	1.44	1.3954	17.09	1.182
1.75	22.64	1	1.75	1.5846	19.95	1.135
2	27.11	1	2	1.9828	26.78	1.012

For nonlinear-elastic model of stage 2 the elements' reinforcement are specified similar in both directions in accordance with column 2 of Table 1. The stress-strain diagram of concrete is assumed to be the three-piecewise-linear under sustained load in correspondence to SP 52-101-2003, i. 5.1. To make any pitch for all pieces of the diagram, the parameters  $\sigma_{b0}$ ,  $\sigma_{bt0}$  were defined by relations  $\sigma_{b0} = 0,95R_b$ ,  $\sigma_{bt0} = 0,95R_{bt}$ , as it was done, for example, in the paper [2]. The stress-strain diagram of steel is assumed to be the two-piecewise-linear in correspondence to SP 52-101-2003, i. 5.2, but with the next differences: horizontal portion has been replaced with the tilted one defined by ordinates of its ends  $\sigma_{s0} = 0,98R_s$ ,  $\sigma_{s2} = 1,02R_s$ ; working resistance  $R_s$  is assumed by SNIP 2.03.01-84\* (see the relationship  $\sigma_{s,SP}$  on Fig. 6).

To provide speed and accuracy of evaluations, we have to specify the upper bound of destruction load limiting the load increase in stepwise algorithm. This boundary load is defined by selection of coefficient  $k$  and is entered in column 4 for

an each reinforcement area. In column 5 there tabulated all real destruction loads, derived by computation.

When processing the models under consideration by stepwise algorithm of LIRA-system, it is executed one-step Newton-Raphson procedure [3, subsec. 7.2], where stiffness matrix, as a matter of fact, is Jacobian matrix for nonlinear system of resolving equations [4, i. 15.10.1]. Refusal to employ iteration process causes the increase of an error of displacement computation, corresponding to increase of current loading, so that result accuracy essentially depends on the loading step value. In the given example the analysis has been done for two successive “local” loadings: in the first one the 67% of total load  $k\tilde{q}$  is implemented with 128 steps of similar value; the remained 33% is divided by 384 steps of second loading. The decrease of the step value up to process termination is necessary to provide an accuracy of computation both with the speed of algorithm. Coefficient  $k$  was selected such that the process terminated not before the middle of runtime of computation of second loading. Such implementation of the algorithm has secured an error small enough on computation of destruction load (see below).

By the results of nonlinear analysis it is evaluated the crack separation distance; to do that we analyze the stress state of the element at the middle of section’s side normal to verified reinforcement direction (hatched element on Fig. 2, c). The crack separation analysis is made for internal moments  $M_x$ ,  $M_y$ ,  $M_{xy}$ , established in the element. The system LIRA 9.x allows to do this analysis automatically — we recommend to specify internal moments and element characteristics in the design subsystem LIR-LARM, then start the computing in the mode of determination of reinforcement. Both with the crack separation distance it will be determined the reinforcement area for given forces, and the affinity of calculated reinforcement area to initial value from the column 2 of Table 1 may be considered as the confirmation of computing accuracy. For the example presented above such affinity is secured.

In the columns 6 and 7 of Table 1 it is given values (4) and (5) obtained at the stage 3. These columns specify the searched function (6). Its plot is presented on Fig. 3, curve 1.



The error estimation of computation is obtained for loads from column 4 of Table 1: for each load it was constructed a sequence of values of destruction load, so that each next load has been obtained through doubling of steps in local loadings. The results of estimation of convergence speed are presented into Table 2, where for each pair of neighbouring members of named sequence it is given the relative deviation

$$\delta_{i-1} = \frac{q_i - q_{i-1}}{q_i}.$$

Let us estimate the destruction load  $q_4$  (for step ratio 128/384). By reason of that the last member in every constructed consequence is neglectable, one can assume the last in raw value of destruction load  $q_5$  (or  $q_6$  for ninth line of the table) to be accurate result. So we have a sample of computing errors of load  $q_4$ :

$$\delta_{\Sigma} = \sum_{i \geq 4} \delta_i. \quad (7)$$

Table 2

$A_y,$ $\text{cm}^2/\text{m}$	$k\tilde{q},$ $\text{ton}/\text{m}^2$	Number $q = q_i$ (ton/m <sup>2</sup> ) for specified ratio of steps in local loadings, error $\delta_i\%$										$\delta_{\Sigma}\%$	
		16/ 48	32/ 96	$\delta_1$ %	64/ 192	$\delta_2\%$	128/ 384	$\delta_3$ %	256/ 768	$\delta_4\%$	512/ 1536		$\delta_5\%$
5.51	0.6	0.5258	0.5216	-0.8	0.5227	0.2	0.5314	1.6	0.5312	-0.04			-0.04
7.27	0.78	0.6513	0.6433	-1.2	0.6392	-0.6	0.6386	-0.1	0.6376	-0.16			-0.16
9.09	0.88	0.759	0.7409	-2.4	0.7318	-1.2	0.7242	-1.0	0.7231	-0.15			-0.15
11.63	1	0.89	0.8591	-3.6	0.8488	-1.2	0.8445	-0.5	0.8423	-0.26			-0.26
14.31	1.08	1.0058	0.9872	-1.9	0.9723	-1.5	0.9677	-0.5	0.9658	-0.20			-0.20
17.15	1.26	1.1387	1.1431	0.4	1.1409	-0.2	1.1550	1.2	1.1555	0.04			0.04
18.65	1.35	1.2108	1.2386	2.2	1.2525	1.1	1.2723	1.6	1.2763	0.03			0.03
20.20	1.44	1.3311	1.3559	1.8	1.3806	1.8	1.3954	1.1	1.3967	0.09			0.09
22.64	1.75	1.5094	1.5334	1.6	1.5665	2.1	1.5846	1.1	1.6177	2.0	1.621	0.20	2.2
27.11	2	1.8762	1.89	0.7	1.9484	3.0	1.9828	1.7	1.9863	0.02			0.02

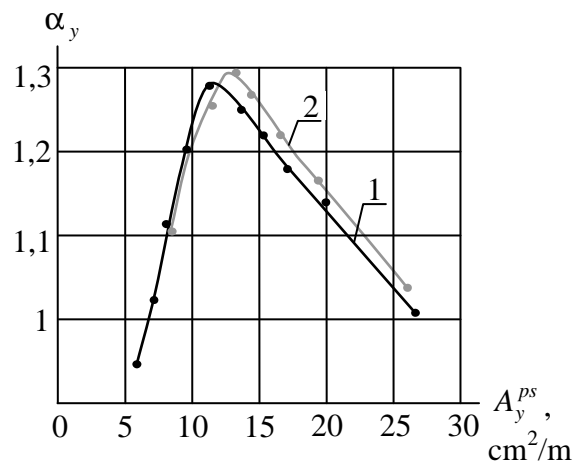


Fig. 3

The error upper bound of destruction load may be determined with the rule of “3 sigma” by sample average  $m$  and sample MSD  $s$  of the sum (7) taken by 10 presented experiments. We have  $\delta_{\max} = |m| + 3s = 2.34\%$ . To find out the calculation relative error of reinforcement area  $A_y^{ps}$ , we note that function (4) is close to linear one, and its diagram may be plotted by the data from the two first columns of Table 1. We easily obtain through consideration of the relation of finite augments  $\Delta A_y^{ps}$  and  $\Delta q$ , that in the expression

$$\frac{\Delta A_y^{\text{to}}}{A_y^{\text{to}}} = \psi \frac{\Delta q}{q}$$

the greatest value of coefficient  $\psi$  is reached at the greatest value  $A_{\max}^{ps} = 22 \text{ cm}^2/\text{m}$  and is equal to  $\psi = 1.2$ . Therefore, the relative error  $\delta_{\max} = 2.34\%$  of a value's  $q$  calculation causes the greatest error  $1.2 \cdot 2.34 \approx 2.8\%$  of evaluated  $A_y^{ps}$  and, respectively, of coefficient  $\alpha_{x(y)}$ . This error is sufficiently small to neglect.

Analogous error estimation for destruction load  $q_3$  (with step ratio 64/192) gives the greatest error  $\delta_{\max} = 5.06\%$ . Corresponding calculation's error of a value  $\alpha_{x(y)}$  is 6.1%. Coefficients  $\alpha_{x(y)}$ , that tabulated into Table S.1 at the paper's supplement, have been calculated with step ratio 128/386, the remained results of supplement have been obtained with ratio 64/192.

For calculation the crack separation it was chosen the element at the middle of an edge of a column cross-section. Note that choosing the element adjacent to the column is not important here by dint of smoothing the internal forces, caused by nonlinear materials properties. On Fig. 4 it is depicted sub-image from the scheme 2,  $c$ , with basic line and diagrams on this one. On the left to the symmetry axis it is plotted the bending moment diagram for armored slab under the load  $q = 0.9677 \text{ ton/m}^2$  (the fifth row of Table 1). It may be seen that moments along the side of section are of not essential difference. For comparison it is depicted on the right the similar diagram obtained through linear calculations for non-armored elements. It may be seen that linear-elastic analysis completes inadequate result. In regards to this, the attempt of

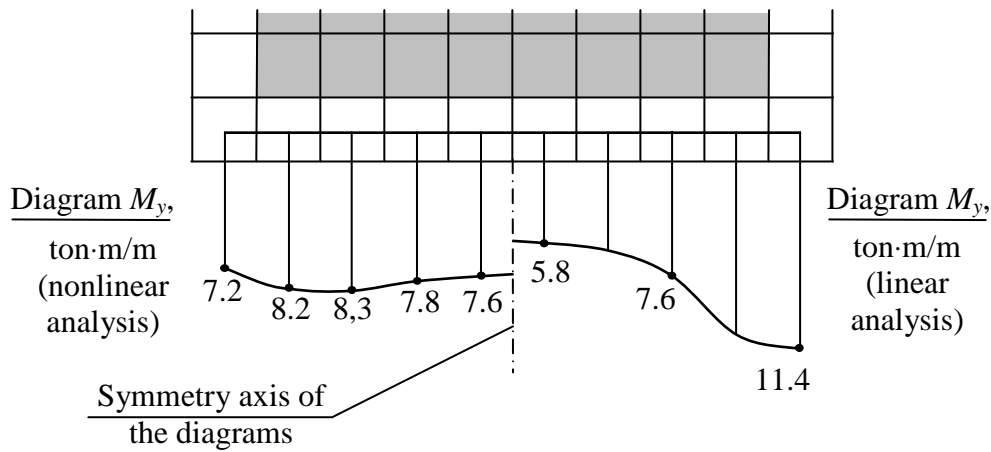


Fig. 4

making reinforcement near supports more precise by condensing FE mesh, might raise error up, for capacity of smoothing the internal forces is lost, while the FEs of big size have this one.

Of the fourth stage's checks we'll consider most labor-intensive check B, which made through analytical model on Fig. 5 (on the left) and respective FE mesh with point support (on the right). The load  $q$  simulates all actual loads on the floor except the load by walling; the load  $P$  makes precise the effect of the load  $q$  at the

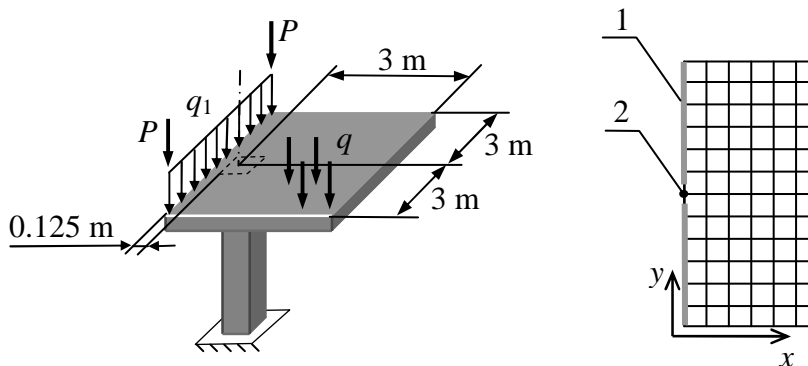


Fig. 5. Analytical model and FE mesh for the check B.  
1 – the line of loading; 2 – the node of point support

spans parallel to slab edge; the load  $q_1$  simulates pressure of walling. In the element adjacent to the point support we can find out 3 internal moments:  $M_y^{wall}$  — bending moment of the walling impact in the cross-section that normal to the edge;  $M_y^{square}$  and  $M_x^{square}$  — bending moments of all remained loadings in specified directions. For the simulated floors of the skeleton under consideration it is evaluated the ranges for every load  $q$ ,  $P$ ,  $q_1$ , producing this forces in the testing model. Besides of the model-

on-the-point-support for described analytical model, we construct nonlinear-elastic model with FE mesh step  $l = 6.25$  cm. This model is used, having loads and reinforcement, to obtain the factor of safety of the structure  $k_{safe}$ , i. e. the coefficient which defines marginal state under loads  $(k_{safe}q, k_{safe}P, k_{safe}q_1)$ . By means of this model for any given value  $A_y^{ps}$  we define the least factor  $k_{safe}$  of the structure, reinforced with allowance for recalculation coefficients (1), under any loads corresponding to accepted reinforcement on the point support, i. e. loads satisfying to the equation

$$A_y^{ps}(q, P, q_1) = A_y^{ps}.$$

Next, by the diagram of the relation  $k_{safe}(A_y^{ps})$  we make a conclusion about passing a check. In considered example the guaranteed factor of safety is no less than 1, that is why recalculation coefficients, defined by the relation 1 on Fig. 3, satisfies to the check B. The checks A and C are completed in similar manner.

On Fig. 3 the curve 2 is plotted for negative-moment reinforcement area  $A'_{x(y)} = 6 \text{ cm}^2/\text{m}$  with step ratio 128/284. By comparison of curves 1 and 2 we note that parameter's  $A'_y$  deviation does not disturb essentially the relation (6).

In the case of rectangular cross-section column  $B \times H$  the technique described above should be generalized by the next complement. The searched relations  $\alpha_y(A_y^{ps})$  and  $\alpha_x(A_x^{ps})$  do not coincide now, and, for beginning, we have to establish their approximations: the relation  $\alpha_y(A_y^{ps})$  is wanted of being established as for a column  $B \times B$ ; the relation  $\alpha_x(A_x^{ps})$  is wanted as for a column  $H \times H$ . After that these relations have to be corrected by the next scheme. In the considered above model of stage 2 we introduce rectangular support of the cross-section  $B \times H$  and specify reinforcement by use of obtained recalculation coefficients  $\alpha_y$  and  $\alpha_x$  for different loads  $q$ . Then we plot the relation  $k_{safe}(q)$  “factor of safety — load” for table-like construction (computing continues until destruction). For typical skeleton these coefficients do not differ significantly from the unit: for instance, it was obtained the value  $k_{safe} \geq$

0.96 for a column  $0.5 \times 0.75$  m and  $h = 20$  cm (see supplement). Having established the relation  $k_{safe}(q)$  and taking into account the plotted distraction pattern we adjust relations  $\alpha_y(A_y^{ps})$ ,  $\alpha_x(A_x^{ps})$  by multiplying factors the such that provide condition  $k_{safe} \geq 1$  on the next recalculation (formulas (S.1) are the examples of adjustment). This computing technology is based on the hypothesis that along each side of upper cross-section of a column, supporting the slab, the SSS of the letter is defined just by the dimension of this side, and is of not valuable dependence on the section's dimension by another direction. Considering the checks A—C of the stage 4 (see above) we note that these checks' technique is applicable to columns of rectangular section with no changes. In the supplement we tabulate results of coefficients  $\alpha$  calculation for different cross-sections of column.

#### 4. About exceeding of reinforcement area by analysis with nonlinear-elastic model

When being calculated reinforcement area by means of nonlinear-elastic model, the virtual distraction could be found out for a reinforcement which provides integrity of the structure in practice. This occurs by the next two reasons.

1. The stepwise calculator of the system LIRA 9.x when applied to the armored slabs, detects distraction on the loss of links to supporting nodes that makes a structure geometrically variable. The loss of link to the support is detected on the state of plastic hinge for any element between the support and the safe part of a structure. The state of structure called plastic hinge in system LIRA may be close to the marginal but not being this. Thus, for instance, plastic hinge arises if the stress in tensile reinforcement becomes greater  $0.8\sigma_s^+$ , where  $\sigma_s^+$  is the greatest stress on the stress-strain diagram of reinforcement tension, and therewith extent of a region of stretched concrete is small enough. That is why it might be detected false destruction on computing analysis.

2. In accordance with SP 52-101-2003, the limpness stress (greatest safety stress) on the armature state diagrams is being conservative because this stress is as-

sumed to be the yield stress (designed stress), whereas distraction is defined by ultimate strength. On Fig. 6 it is depicted 3 diagrams of tension of reinforcement A-III:  $\sigma_{s,SP}(\epsilon)$  — diagram by SP 52-101-2003;  $\sigma_{s,ex}(\epsilon)$  — experimental diagram from the book [5], the such that the yield stress  $\sigma_y$  and ultimate stress  $\sigma_u$  correspond to GOST 5781-82;  $\sigma_{s,test}(\epsilon)$  — piecewise-linear diagram, inclosing hardening segment. The lat-

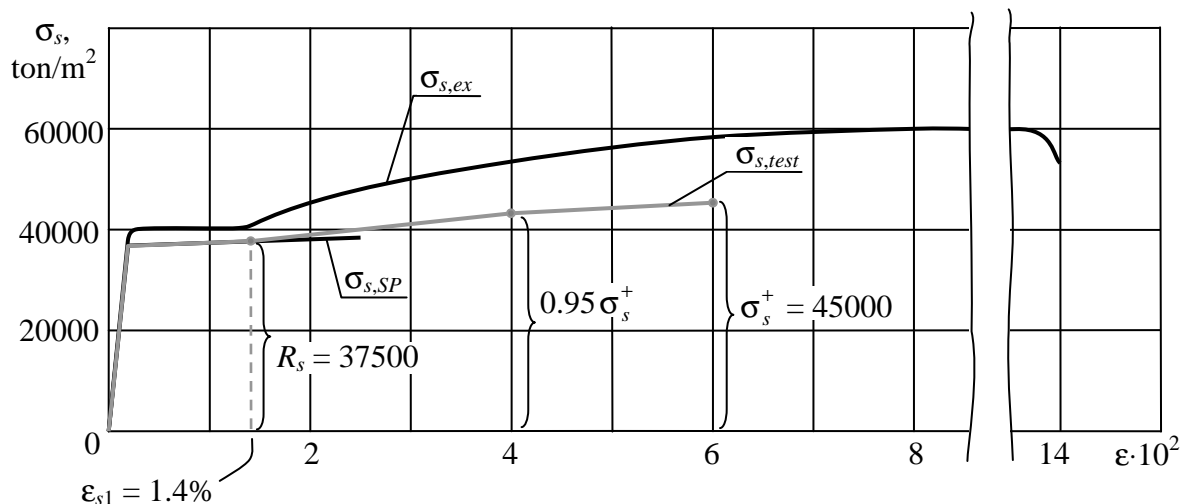


Fig. 6

ter diagram has been used in repeated analysis with nonlinear-elastic models, that aiming to obtain lower reinforcement area providing structure strength, yet violating the requirements of SP 52-101-2003. This testing diagram is obtained by extrapolation of diagram  $\sigma_{s,SP}$  in such manner, that from point  $\epsilon_{s1}$  the ratio  $\sigma_{s,ex}(\epsilon)/\sigma_{s,test}(\epsilon)$  would increase from 1.07 (i. e. from reinforcement reliability coefficient by SNIP 2.03.01-84\*) up to 4/3 with ultimate strain 6%. This ultimate strain is of lesser value then relative stretch  $\delta_5 = 14\%$  by GOST 5781-82 (1994). Owing to the listed peculiarities of testing diagram the results of analysis using the latter are being sufficiently reliable.

Being calculated SSS by means of nonlinear-elastic model elaborated for the problem considered in Sect. 3, one confirms integrity of the structure with unit coefficients  $\alpha_{x(y)}$ . This result accounts for the integrity of reinforced monolithic structures designed with no holding of required FE mesh step — namely, because of possible analysis errors the real state of reinforcement might change to tensile hardening zone

(behind the yield point), when the crack separation being out of limit but there is no destruction of structure.

Remark. Diagram of compression of structural steel is in close agreement with diagram of tension on strain range up to hardening, and for greater strains (by module) the compression stress is greater than tension stress [6]; in consequence of this we assume the diagram of reinforcement state being symmetrical.

### Results.

On analysis of monolithic slab reinforcement by means of FE model with point supports, we have to take into account the relation between obtained results and FE mesh step.

The amendment of reinforcement area in the vicinity of point supports is attained with recalculation coefficients for reinforcement area, which depend on FE mesh step and may be tabulated.

Analysis by SP 52-101-2003 does not take into account additional strength of structure, corresponding to working state of reinforcement at the hardening zone of diagram of state.

## REFERENCES

1. Clovanich, S.F., Mironenko, I.N, Finite element method in reinforced concrete mechanics. Odessa, Odessa National Marine Univers., 2007, 110 p. (In Russian)
2. Rusakov, A.I., The Technique of Experienced-Theoretical Estimation of Deflections of Monolithic Armored Floor. Industrial and Civil Engineering, 2010, No. 3, pp. 28-32. (in Russian)
3. Strelets-Streletski, E.B., and others, LIRA 9.2. User Manual. Basics. The textbook. Edited by Gorodetski A.S., Kiev, Fact, 2005, 145 p. (in Russian)
4. ANSYS, Inc. Theory. Release 5.7. Edited by Peter Kohnke, ANSYS, Inc., Cansonsburg, 2001, 1264 p.

5. Bondarenko, V.M., Bakirov, R.O., Nazarenko, V.G., Rimshin, V.I., Reinforced Concrete and Stone Constructions. Edited by Bondarenko V.M., Moscow, Visshaja shkola, 2002, 876 p. (in Russian)
6. Rusakov, A.I., Course of Lectures on Strength of Materials. Rostov-on-Don, "Kniga", 2004, 326 p. (in Russian)

## SUPPLEMENT

RELATIONS  $\alpha_y = \alpha_y(A_y^{ps})$ ,  $\alpha_x = \alpha_x(A_x^{ps})$   
CORRESPONDING TO FE MESH OF CELL  $l = 50$  cm

**In all tabulated relations below, for the intermediate argument's value the function has to be established by linear interpolation.**

The analysis conditions are defined at the first paragraph of sect. 3 except by the next:  $A'_{x(y)} = 4$  cm<sup>2</sup>/m; the column cross-section dimensions are given below.

Table S.1

**Column section  $B \times H = 0.5 \times 0.5$  m**

Variable	Variables' values for dimensionality [ $A_y^{ps}$ ] = cm <sup>2</sup> /m				
$A_y^{ps}$	5	6.5	10	12.5	25
$\alpha_y$	0.9	1	1.23	1.29	1.15

Table S.2

**Column section  $B \times H = 0.75 \times 0.75$  m**

Variable	Variables' values for dimensionality [ $A_y^{ps}$ ] = cm <sup>2</sup> /m				
$A_y^{ps}$	5	12	16.5	19	25
$\alpha_y$	0.8	0.96	1.02	1.01	0.96

**Column section  $B \times H = 0.5 \times 0.75$  m:** the relations searched are obtained by means of tables S.1 and S.2 after correction as follows:

$$\alpha_y^{0.5 \times 0.75} = 1.02 \alpha_y^{0.5 \times 0.5}(A_y^{ps}); \quad \alpha_x^{0.5 \times 0.75} = 1.05 \alpha_x^{0.75 \times 0.75}(A_x^{ps}). \quad (S.1)$$

— Coefficients are calculated for the column location inside the floor grid.

Table S.3

**Column section  $B \times H = 0.375 \times 0.375$  m**

Variable	Variables' values for dimensionality [ $A_y^{ps}$ ] = cm <sup>2</sup> /m					
$A_y^{ps}$	5.5	8.5	11	14	17.5	22.5
$\alpha_y$	1.00	1.26	1.31	1.32	1.26	1.20